DOI: 10.1002/ejoc.200600368

Predicting Enantioselectivity: Computation as an Efficient "Experimental" Tool for Probing Enantioselectivity

Andrea Ragusa,[a][‡] Joseph M. Hayes,*[b][‡‡] Mark E. Light,[a] and Jeremy D. Kilburn*[a]

Keywords: Enantioselectivity / Host–guest systems / Molecular recognition / Molecular modelling / MINTA

As a result of the accurate agreement between computation and experiment obtained using default forcefield parameters, the MMFFs forcefield together with a Monte Carlo conformational search method (MCMM/LMCS) and the MINTA free-energy calculation algorithm has been used to probe the enantioselective potential of a new macrocyclic receptor, hence saving time and money on costly experimental procedures.

Introduction

The development of effective experimental protocols for the rapid and efficient prediction of new candidate synthetic receptors for enantioselective discrimination has long been a major topic in supramolecular chemistry. Computational chemistry in the past has served mostly as a useful tool for the study of binding modes, and has helped in the rational design of new chiral receptors.[1] However, there are few examples of computations performed able to reproduce experimental binding results accurately, and consistently without either extensive forcefield reparametrisation[2,3] and/or highly demanding computational calculations;[4] even fewer which use computation as a successful prediction tool following computational/experimental cross validation of results. Still and co-workers succeeded in calculating the selectivity of a podand ionophore for enantiomeric α-amino acid derived substrates.[4a] However, the accurate prediction of the binding free energy differences ($\Delta\Delta G^{L-D}$) using free energy perturbation (FEP) was a demanding task requiring time-consuming calculations and high-level computational power. Recently, the much faster MINTA (mode integration) algorithm[5] has given impressive results for the prediction of relative binding free energies in chiral separation studies.[3,6,7] Furthermore, application of MINTA to calculate the *A* value of methylcyclohexane was at least 43 times faster than FEP.[5]

MINTA involves the direct computation of the configuration integral as a sum of the contributions from low energy conformational states.[5] In contrast to the "mining minima" algorithm which just uses the torsion angles,[8] MINTA calculates the configuration integral over all degrees of freedom using an effective Hessian to integrate in normal mode space for each single conformer. Free energy calculations using MINTA are ideally necessarily preceded by an exhaustive conformation search to locate all low energy conformations, which is best achieved using a Monte Carlo (MC) algorithm. Success of MINTA is therefore limited by the success of the conformational search but also by the quality of the forcefield parameters used.[3] MINTA's neglect of rotational and translational contributions to the configuration integral has been criticised,[9,10] but has not been a problem in all chiral separation studies with MINTA reported to date.[3,6,7] Nevertheless, it remains to be seen how MINTA will perform when the binding of sterically more diverse ligands than enantiomers are investigated.

Here we present a combined computational and experimental study on the structural and enantiodiscrimination properties of the new rigid macrocyclic receptor **1** with amino acid guests, showing unusually accurate agreement between the two methods. Supported by crystallographic data and NMR titration experiment data, the computational procedures employed were able to reproduce with high accuracy the experimental data using default MMFFs forcefield parameters,[11,12] conformational searches and the MINTA free energy calculation algorithm. The rigidity and simplicity of the system minimises potential errors due to the forcefield or due to inadequate sampling of the conformational space for the subsequent free energy simulations using MINTA.[13,14] The MMFFs forcefield was chosen due to its success in modelling the more flexible dimer analogue of receptor **1** where other forcefields (AMBER* and OPLS-AA) were also tested for their suitability.[1] Put simply, the systems we choose to model should in theory pose few computational problems – a rigid macrocycle containing well-parameterised subunits and functional groups, and simi-

[a] School of Chemistry, University of Southampton, Southampton, SO17 1BJ, UK
E-mail: jdk1@soton.ac.uk
[b] Anterio Consult and Research GmbH, Augustaanlage 26, 68165, Mannheim, Germany
[‡] Current address: Laboratory of Glyconanotechnology, IIQ, CSIC, Calle Américo Vespucio 49, 41092 Seville, Spain
[‡‡] Current address: Departament de Química, Universitat Autònoma de Barcelona, 08193 Bellaterra (Barcelona), Spain, E-mail: joe@klingon.uab.es

larly, well-parameterised simple amino acids. Significantly, the computational/experimental comparison of initial data was so impressive, that the demanding experimental procedures were abandoned in favour of screening receptor **1** with a series of amino acids using time-efficient MC conformational searches and MINTA free energy calculations of $\Delta\Delta G^{L-D}$. Computation was hence employed as the screening tool for enantioselectivity saving significant experimental time and reducing laboratory costs.

Results and Discussion

Macrocycle **1** represents the monomer analogue of an already reported receptor.[1,15] It possesses a thiourea moiety as the main carboxylate binding site, and additional hydrogen bonding is provided by two amide groups. The bulky phenyl rings should allow enantioselective discrimination. In Figure 1 the proposed/expected mode of binding is presented.

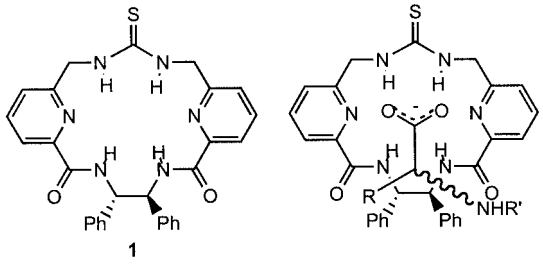

Figure 1. Macrocyclic receptor **1** and the proposed mode of binding. PG = protecting group.

Conformational organisation of the macrocycle was determined in the solid state by X-ray crystallography, showing that the receptor possesses a very rigid structure. In Figure 2 the X-ray crystal structure of the macrocycle is shown (sample recrystallised from DMSO), which includes a single DMSO molecule in order to maximise hydrogen-bonding interactions between the DMSO oxygen atom and the four macrocycle NH units (2.03–2.37 Å).[16] Intramolecular hydrogen bonds between the four NH units and the pyridine nitrogen atoms are also observed. ^{1}H NMR analysis agrees with the conformation in the solid state. No substantial changes to the ^{1}H NMR spectrum were observed moving from the apolar $CDCl_3$ to the more competitive [D_6]DMSO except for the thiourea NH signal, which shifts considerably downfield (from $\delta \approx 7.5$ ppm in $CDCl_3$ to $\delta = 8.72$ ppm in [D_6]DMSO) as a consequence of hydrogen bonding to the solvent molecule.

Experimental evaluation of the binding properties of acetyl (Ac) or *tert*-butoxycarbonyl (Boc) protected amino acids to macrocycle **1** using NMR titration experiments in $CDCl_3$ showed that the receptor binds them strongly, forming the expected 1:1 host–guest complex with all guests tested (Table 1). Association constants range from $4.9 \cdot 10^2$ to $1.9 \cdot 10^3$ M^{-1}, indicating strong interaction between the receptor and the guest, and in all cases a considerable downfield shift of the thiourea NH proton signal was observed in the ^{1}H NMR spectra. However, the enantioselectivity ($\Delta\Delta G^{L-D}$) observed using these amino acids was not substantial. NMR titration experiments were also attempted in the more competitive [D_6]DMSO, but no binding was noticed in this solvent.

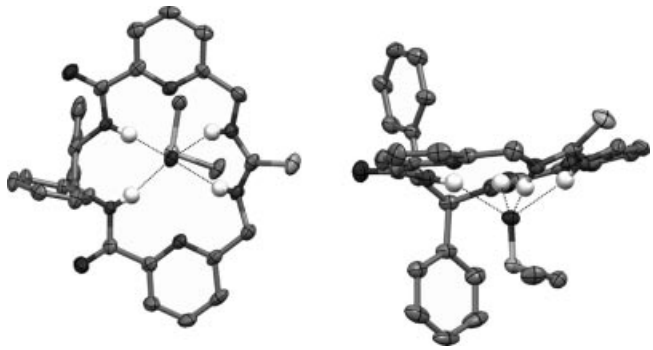

Figure 2. X-ray crystal structure of macrocycle **1** in DMSO showing complexation of a solvent molecule.

Table 1. Experimental binding constants (K_a) and free energies of complexation ($-\Delta G$) for the 1:1 complexes formed between macrocycle **1** and tetrabutylammonium salts of *N*-protected amino acids in $CDCl_3$ at 298 K.

Guest	K_a [M^{-1}]	$-\Delta G$ [kJ mol^{-1}]	$\Delta\Delta G^{L-D}$ [kJ mol^{-1}]
N-Boc-L-Phe	$8.87 \cdot 10^2$	16.8	–0.3
N-Boc-D-Phe	$7.96 \cdot 10^2$	16.5	
N-Ac-L-Phe	$7.74 \cdot 10^2$	16.5	–1.2
N-Ac-D-Phe	$4.86 \cdot 10^2$	15.3	
N-Ac-L-Gln	$1.47 \cdot 10^3$	18.1	+0.6
N-Ac-D-Gln	$1.94 \cdot 10^3$	18.7	

Molecular dynamics (MD) simulations (300 K) in explicit DMSO were performed, using MacroModel 8.1,[17] to investigate the conformational preferences of macrocycle **1**. The calculations revealed the macrocycle to be a highly rigid structure with a preference for binding of a single DMSO molecule through hydrogen bonding to the oxygen atom, in agreement with the solid-state structure (Figure 2). Furthermore, the RMS distance between heavy atoms for the average minimised trajectory conformation from the MD simulations and the X-ray crystal conformation is just 0.5 Å. This reduced to ca. 0.3 Å on excluding the phenyl ring heavy atoms. Superimposition of the DMSO X-ray crystal structure and average minimised MD conformation are shown in Figure 3. The MD simulations also revealed that the average enthalpy with a receptor-bound amino acid (*N*-Ac-alanine) in DMSO is much higher (46 kJ mol^{-1}) than when a DMSO molecule itself is coordinated. Computation therefore suggests that the energetic cost of breaking the hydrogen bonds with the solvent molecule is not compensated for by the binding of a guest amino acid, which explains why no binding in DMSO was experimentally observed. Instead the small DMSO molecule fits particularly

well inside the cavity of the receptor with little steric clash with the receptor's backbone, as already observed in the solid-state structure.

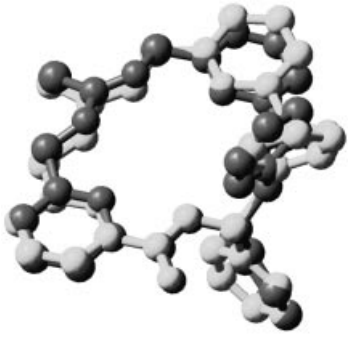

Figure 3. Superimposition of an average minimised macrocyclic conformation from MD simulations in DMSO (light grey) and the X-ray crystal structure in DMSO (dark grey).

The mixed mode Monte Carlo Multiple Minima/Low-Mode Conformational Search (MCMM/LMCS) algorithm[18–20] was used to study the binding of macrocycle **1** and *N*-protected α-amino acids in $CHCl_3$ solvent, and to generate the conformations for calculation of the free energies using MINTA. The solvent effects were included using the implicit GB/SA continuum model.[21] Excellent agreement with experiment for the enantioselectivity was observed in all cases (Table 2). The direction of enantioselectivity is predicted correctly in each case, but more impressive is the accuracy of the relative ordering of the computational $\Delta\Delta G^{L-D}$ value compared to experiment. We note that the errors for the computed $\Delta\Delta G^{L-D}$ values are not small (±1.2–1.4 kJ mol^{-1}) and could be reduced by employing a greater number of sampling points per block (see Experimental Section).[22] However, within the bounds of the current errors the experimental $\Delta\Delta G^{L-D}$ trend is still followed and reducing the $\Delta\Delta G^{L-D}$ errors would not change this key result or lead to new information. A different mode of binding was obtained compared to that proposed initially (Figure 1). The modelling results indicate that the carboxylate group is bound by four hydrogen bonds, one from each NH group of the macrocycle to just one of the carboxylate oxygen atoms, with additional interactions in most cases between the amino acid NH group and a macrocycle pyridine nitrogen atom (Figure 4). An intramolecular hydrogen bond from the amino acid NH group to the bound carboxylate oxygen atom is also often present. So even for amino acids, as was the case for binding of a DMSO molecule, the receptor shows a preference for binding of just one oxygen atom deep within the macrocycle cavity to maximise the hydrogen bond contacts. With the exception of *N*-Ac-glutamine, the binding of the D-enantiomer is less favourable, as the host–guest complex does not have the additional interaction between the amino acid NH group and the pyridine nitrogen atom. It is also clear that in all cases the main enthalpic contribution to chiral discrimination is limited to steric hindrance of entry of the carboxylate group into the macrocyclic cavity. However, as seen by the computed large entropic contribution to the enantioselectivity for binding of *N*-Ac-phenylalanine, entropic effects appear to often play a major role in the overall selectivity obtained. These entropic effects are well accounted for using MINTA.

Table 2. Comparison between computational and experimental results for enantioselectivity predictions in $CHCl_3$.[a]

Guest	Experiment	Computation		
	$\Delta\Delta G^{L-D}$	$\Delta\Delta H^{L-D}$[b]	$\Delta\Delta G^{L-D}$[c]	$\Delta\Delta S^{L-D}$[d]
N-Ac-Phe	–1.3	–1.4	–4.7	–3.3
N-Boc-Phe	–0.2	–1.3	–1.4	–0.1
N-Ac-Gln	+0.4	+2.7	+2.3	–0.4

[a] In kJ mol^{-1}. [b] At 0 K. Calculated from difference in energies between global energy L- and D-bound complexes from the MCMM/LMCS conformational searches. [c] As calculated using MINTA at 300 K. Error in $\Delta\Delta G^{L-D}$ values is ± 1.2–1.4 kJ mol^{-1}. [d] Entropy estimates calculated as the difference between $\Delta\Delta H^{L-D}$ (0 K) and $\Delta\Delta G^{L-D}$ (300 K).

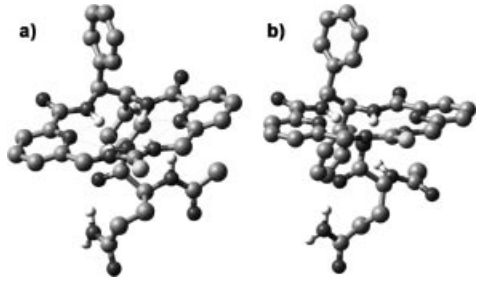

Figure 4. Molecular modelling global minimum conformations obtained for (a) the L- and (b) the D-bound complexes of *N*-Ac-glutamine with macrocycle **1** in $CHCl_3$.

On the basis of the excellent results obtained using computation, the experimental procedures were abandoned, and we proceeded to screen macrocycle **1** with further *N*-Ac- and *N*-Boc-protected amino acids for better enantioselectivity using the conformational search – MINTA approach. The results of the screening are shown in Table 3. Our calculations determined *N*-Ac-alanine (–4.9 kJ mol^{-1}) and *N*-Ac-asparagine (–4.8 kJ mol^{-1}) to have similar selec-

Table 3. Computational screening of a series of amino acids for enantioselectivity on binding to macrocycle **1** in $CHCl_3$.[a]

Guest	Computation		
	$\Delta\Delta H^{L-D}$[b]	$\Delta\Delta G^{L-D}$[c]	$\Delta\Delta S^{L-D}$[d]
N-Ac-Ala	–4.6	–4.9	–0.3
N-Boc-Ala	–3.0	–1.4	+1.6
N-Ac-Ser	–0.3	–0.7	–0.4
N-Boc-Ser	–0.9	–2.0	–1.1
N-Ac-Val	–0.8	–0.6	+0.2
N-Boc-Val	+0.3	+0.3	0.0
N-Ac-Asp	–4.1	–4.8	–0.7
N-Boc-Asp	–2.8	–1.9	+0.9
N-Ac-Tyr	–2.0	–1.4	+0.6
N-Ac-Try	+1.2	–1.2	–2.4

[a] All values are in kJ mol^{-1}. [b] At 0 K. Calculated from difference in energies between global energy L- and D-bound complexes from the MCMM/LMCS conformational searches. [c] As calculated using MINTA at 300 K. Error in $\Delta\Delta G^{L-D}$ values is ± 1.2–1.4 kJ mol^{-1}. [d] Entropy estimates calculated as the difference between $\Delta\Delta H^{L-D}$ (0 K) and $\Delta\Delta G^{L-D}$ (300 K).

tivity to *N*-Ac-phenylalanine (–4.7 kJ mol^{-1}), but no amino acid was found to have greater enantioselectivity with macrocycle **1**. So, although computational time was lost in the screening process of the amino acids in Table 3, it was a considerable saving compared to alternatively pursuing the financially and time-costly experimental procedures. Indeed, based on this study, this approach to determining enantioselectivity is now a very attractive option for us which may in the future lead to a more satisfying result.

Conclusions

Concluding, a new macrocyclic receptor has been synthesised and its enantioselective properties investigated by NMR titration experiments. Default MMFFs forcefield parameters together with conformational search methods (MCMM/LMCS and MD) and the MINTA free-energy algorithm were particular efficient in reproducing experimental results. The agreement was so impressive that standard experimental protocols were abandoned in favour of computation for further screening of the macrocycle's enantioselective potential. We believe that the rigidity of the macrocycle was crucial in such agreement being obtained. Systems that are more flexible have greater sensitivity to accurate forcefield parameters and conformational search protocols employed. Nevertheless, with the release of the highly awaited polarisable forcefields on the horizon,[23] these results would indicate that such accuracy in enantioselective predictions in the future will not be so rare. Indeed, substituting demanding experimental procedures with computation as a tool for predicting enantioselectivities with algorithms such as MINTA could yet become more commonplace in chiral separation studies.

The macrocyclic behaviour (conformational and binding properties) in other solvents is being studied, as are further computational studies with other amino acid derivatives. These results will be reported in due course.

Experimental Section

Molecular Modeling: For the MCMM/LMCS conformational searches, global ligand translations were included in the binding pocket of the receptor. In total, 2–5 torsions were randomly selected and adjusted each MCMM step, with a 1:1 ratio of MC torsional moves and/or ligand translation to the LMCS low mode moves. 3000 steps were performed for each receptor–enantiomer complex with an energy window of 50 kJ mol^{-1} above the global minimum used for saving conformations. For the MINTA free energy calculation, binding conformations generated from the conformational searches were first reminimised using the MacroModel "multiple minimisation" algorithm. The resulting conformations were used in separate free energy calculations of $G^{R\text{-}L}$ and $G^{R\text{-}D}$ at 300 K for receptor-bound L (R-L) and D (R-D) complexes, respectively. MINTA integrals were calculated as block averages with 10×1000 energy evaluations per conformation. Numerical integration in all degrees of freedom was used throughout, with hard and soft limits of 1 Å and 3 units of standard deviation used, respectively, for sampling along the normal modes. Finally, as the isolated enantiomeric free energies are the same ($G^{L} = G^{D}$), the binding free energy difference $\Delta\Delta G^{L-D}$ was calculated simply as $\Delta\Delta G^{L-D} = G^{R\text{-}L} - G^{R\text{-}D}$. MD simulations in explicit DMSO were performed at 300 K using the standard constant *T* velocity Verlet algorithm and MacroModel "substructures" (shells). Two different starting conformations were used: (a) macrocycle and unbound *N*-Ac-L-alanine enantiomer system (bound DMSO molecule) and (b) macrocycle with bound *N*-Ac-L-alanine. Systems (a) and (b) were prepared by introducing the macrocycle and enantiomer to a previously equilibrated DMSO system at experimental density (1.096 g cm^{-3}).[1,24] Overlapping solvent molecules and those giving rise to repulsive interactions were then deleted. Systems (a) and (b) contained 3 substructures (shells): unconstrained inner shell (macrocycle, *N*-Ac-L-alanine and 65 DMSO molecules); semi-frozen middle solvation shell (32 DMSO molecules); and frozen outer solvation shell (277 DMSO molecules). The semi- and fully frozen shells were identical for both systems so that the thermodynamic (enthalpy) data from the MD simulations (a) and (b) could be directly compared. Short minimisations (5000 steps, PRCG algorithm) were performed followed by full MD simulations (2 ns equilibration; 30 ns data collection) using a timestep of 1 fs. Conformations from MD trajectory (a) with bound DMSO were clustered into groups of similar conformation. The representative conformation from the largest cluster was minimised (1000 steps, TNCG algorithm) and compared with the DMSO crystal structure. Clustering calculations were performed using NMRclust 1.2.[25] All other calculations were performed using MacroModel 8.1[17] and the default MMFFs forcefield.[11,12]

Acknowledgments

We thank the European Commission (TMR Network grant "Enantioselective Separations" ERB FMRX-CT-98-0233) for financial support, postgraduate fellowships (A. R.) and post-doctoral fellowships (J. M. H.).

[1] A. Ragusa, S. Rossi, J. M. Hayes, M. Stein, J. D. Kilburn, *Chem. Eur. J.* **2005**, *11*, 5674–5688.
[2] R. H. Henchman, J. D. Kilburn, D. L. Turner, J. W. Essex, *J. Phys. Chem. B* **2004**, *108*, 17571–17582.
[3] J. M. Hayes, M. Stein, J. Weiser, *J. Phys. Chem. A* **2004**, *108*, 3572–3580.
[4] a) M. T. Burger, A. Armstrong, F. Guarnieri, D. Q. McDonald, W. C. Still, *J. Am. Chem. Soc.* **1994**, *116*, 3593–3594; b) N. M. Maier, S. Schefzick, G. M. Lombardo, M. Feliz, K. Rissanen, W. Lindner, K. B. Lipkowitz, *J. Am. Chem. Soc.* **2002**, *124*, 8611–8629; c) C. Czerwenka, M. M. Zhang, H. Kahlig, N. M. Maier, K. Lipkowitz, W. Lindner, *J. Org. Chem.* **2003**, *68*, 8315–8327; d) Y. Choi, S. Jung, *Carbohydr. Res.* **2004**, *339*, 1961–1966.
[5] a) I. Kolossváry, *J. Phys. Chem. A* **1997**, *101*, 9900–9905; b) I. Kolossváry, US Patent, 08/940145, **1997**.
[6] A. Del Rio, J. M. Hayes, M. Stein, P. Piras, C. Roussel, *Chirality* **2004**, *16*, S1–S11.
[7] I. Kolossváry, *J. Am. Chem. Soc.* **1997**, *119*, 10233–10234.
[8] M. S. Head, J. A. Given, M. K. Gilson, *J. Phys. Chem. A* **1997**, *101*, 1609–1618.
[9] M. J. Potter, M. K. Gilson, *J. Phys. Chem. A* **2002**, *106*, 563–566.
[10] C.-E. Chang, M. J. Potter, M. K. Gilson, *J. Phys. Chem. B* **2003**, *107*, 1048–1055.
[11] a) T. A. Halgren, *J. Comput. Chem.* **1996**, *17*, 490–519; b) T. A. Halgren, *J. Comput. Chem.* **1996**, *17*, 520–552; c) T. A. Halgren, *J. Comput. Chem.* **1996**, *17*, 553–586; d) T. A. Halgren, *J. Comput. Chem.* **1996**, *17*, 616–641; e) T. A. Halgren, R. B. Nachbar, *J. Comput. Chem.* **1996**, *17*, 587–615.

[12] a) T. A. Halgren, *J. Comput. Chem.* **1999**, *20*, 720–729; b) T. A. Halgren, *J. Comput. Chem.* **1999**, *20*, 730–748.
[13] P. Kollman, *Chem. Rev.* **1993**, *93*, 2395–2417.
[14] P. A. Kollman, *Acc. Chem. Res.* **1996**, *29*, 461–469.
[15] a) S. Rossi, G. M. Kyne, D. L. Turner, N. J. Wells, J. D. Kilburn, *Angew. Chem.* **2002**, *114*, 4407–4409; b) S. Rossi, G. M. Kyne, D. L. Turner, N. J. Wells, J. D. Kilburn, *Angew. Chem. Int. Ed.* **2002**, *41*, 4233–4236.
[16] Single crystal diffraction study: Data were collected with a Bruker Nonius KappaCCD mounted at the window of an FR591 molybdenum rotating anode according to standard procedures. Corrections for absorption and related effects were performed using SADABS V2.10 (G. M. Sheldrick, **2003**), the structure was solved and refined using SHELX97-2 (G. M. Sheldrick, Institut für Anorganische Chemie der Universität Göttingen, Germany, **1998**). Crystal data for **1**: $C_{31}H_{32}N_6O_3S_2$, Mr = 600.75, T = 120(2) K, λ = 0.71073 Å, monoclinic, space group $P2_1$, a = 17.630(5), b = 9.1613(13), c = 18.493(4) Å, β = 98.75(3)°, V = 2952.2(11) Å^3, $\rho_{calcd.}$ = 1.352 g cm^{-3}, μ = 0.224 mm^{-1}, Z = 4 (2 molecules), reflections collected: 20190, independent reflections: 10195 (R_{int} = 0.0706), final R indices [$I > 2\sigma I$]: R_1 = 0.0605, wR_2 = 0.1188, R indices (all data): R_1 = 0.1050. wR_2 = 0.1362. CCDC-292461 contains the supplementary crystallographic data for this paper. These data can be obtained free of charge from The Cambridge Crystallographic Data Centre via www.ccdc.cam.ac.uk/data_request/cif.
[17] a) MacroModel version 8.1, Schrodinger, LLC, New York, NY, **2003**; b) F. Mohamadi, N. G. J. Richards, W. C. Guida, R. Liskamp, M. Lipton, C. Caufield, G. Chang, T. Henrickson, W. C. Still, *J. Comput. Chem.* **1990**, *11*, 440–467.
[18] G. Chang, W. C. Guida, W. C. Still, *J. Am. Chem. Soc.* **1989**, *111*, 4379–4386.
[19] M. Saunders, K. N. Houk, Y. D. Wu, W. C. Still, M. Lipton, G. Chang, W. C. Guida, *J. Am. Chem. Soc.* **1990**, *112*, 1419–1427.
[20] I. Kolossváry, W. C. Guida, *J. Am. Chem. Soc.* **1996**, *118*, 5011–5019.
[21] W. C. Still, A. Tempczyk, R. C. Cawley, T. Hendrickson, *J. Am. Chem. Soc.* **1990**, *112*, 6127–6129.
[22] MINTA gives a statistical error estimate calculated from block averages.[5] This error decreases with increasing number (N) of sampling points for single block sampling [≈ 1/sqrt(N)]; however, using multiple blocks as MINTA does, yields a smaller error. Running MINTA with more sampling points/blocks allows for calculation of any free energy value with high accuracy.
[23] J. R. Maple, Y. Cao, W. Damm, T. A. Halgren, G. A. Kaminski, L. Y. Zhang, R. A. Friesner, *J. Chem. Theory Comput.* **2005**, *1*, 694–715.
[24] www.chemfinder.com.
[25] a) L. A. Kelley, S. P. Gardner, M. J. Sutcliffe, *Protein Eng.* **1996**, *9*, 1063–1065; b) http://neon.chem.le.ac.uk/nmr.clust/.

Received: April 27, 2006
Published Online: July 10, 2006

